Titre: Title:	Self-healing UV curable acrylate coatings for wood finishing system, part 1: impact of the formulation on self-healing efficiency
Auteurs: Authors:	Chloé Paquet, Thomas Schmitt, Jolanta-Ewa Sapieha, Jean-François Morin, & Véronic Landry
Date:	2020
Type:	Article de revue / Article
Référence: Citation:	Paquet, C., Schmitt, T., Sapieha, J.-E., Morin, J.-F., & Landry, V. (2020). Self-healing UV curable acrylate coatings for wood finishing system, part 1: impact of the formulation on self-healing efficiency. Coatings, 10(8), 770 (19 pages). https://doi.org/10.3390/coatings10080770

URL de PolyPublie: PolyPublie URL:	https://publications.polymtl.ca/9376/
Version:	Version officielle de l'éditeur / Published version Révisé par les pairs / Refereed
Conditions d'utilisation: Terms of Use:	Creative Commons Attribution 4.0 International (CC BY)

Titre de la revue: Journal Title:	Coatings (vol. 10, no. 8)
Maison d'édition: Publisher:	MDPI
URL officiel: Official URL:	https://doi.org/10.3390/coatings10080770
Mention légale: Legal notice:	© 2020 by the authors. Licensee MDPI, Basel, Switzerland. This article is an open access article distributed under the terms and conditions of the Creative Commons Attribution (CC BY) license (http://creativecommons.org/licenses/by/4.0/).

Article

Self-Healing UV Curable Acrylate Coatings for Wood Finishing System, Part 1: Impact of the Formulation on Self-Healing Efficiency

Chloé Paquet [1], Thomas Schmitt [2], Jolanta E. Klemberg-Sapieha [2], Jean-François Morin [3] and Véronic Landry [1,*]

[1] Département des Sciences du Bois et de la Forêt, Chaire de Recherche Industrielle CRSNG–Canlak en Finition des Produits du Bois d'Intérieur (CRIF), Université Laval, Québec, QC G1V 0A6, Canada; chloe.paquet.1@ulaval.ca

[2] Département de Génie Physique, Polytechnique Montréal, Montréal, QC H3T 1J4, Canada; thomas.schmitt@polymtl.ca (T.S.); jsapieha@polymtl.ca (J.E.K.-S.)

[3] Département de Chimie et Centre de Recherche sur les Matériaux Avancés (CERMA), Université Laval, Québec, QC G1V 0A6, Canada; jean-francois.morin@chm.ulaval.ca

* Correspondence: veronic.landry@sbf.ulaval.ca; Tel.: +1-418-656-2131 (ext. 402314)

check for updates

Abstract: In the wood flooring sector, good surface mechanical properties, such as abrasion and scratch resistance, are prerequisite. Surface wood protection is provided by finishing systems. Despite coating improvement, scratches formation on wood flooring is unavoidable. A new approach to increase service life is to confer the self-healing property to the finishing system. The most common coatings used for prefinished wood flooring are acrylate UV curable 100% solids coatings. They usually have good mechanical properties and high cross-linking density. The objective of this study was to develop and evaluate an intrinsic self-healing formulation, which is applicable to wood flooring. For this purpose, acrylate formulations were developed with monomers and oligomers carrying hydroxyl groups. To meet the requirements of wood application, hardness, and polymerization conversion of coatings were evaluated. König pendulum damping tests provide information on coating hardness and flexibility. Results around 80 oscillations is acceptable for UV curable wood sealer. The chemical composition was studied by FT-IR spectroscopy while dynamical mechanical analysis (DMA) was performed to determine glass transition temperature and cross-linking density. The self-healing behavior was evaluated by gloss and scratch depth measurements. The formulation's composition impacted the hydrogen binding quantity, the conversion, the T_g and the cross-linking density. The (hydroxyethyl)methacrylate (HEMA) monomer provided self-healing and acrylated allophanate oligomer allowed self-healing and cross-linking. This study demonstrated that it is possible to combine high cross-linking density and self-healing property, using components with low steric hindrance.

Keywords: acrylate; UV curable; self-healing; hydrogen bonds; cross-linking

1. Introduction

One of the main challenges of interior wood products is to sustain mechanical solicitation causing scratches. To maintain good aesthetics of wooden planks over their entire service life, the development of more efficient finishing systems is required. The level of protection needed depends on the final application. In the case of wood flooring, high mechanical resistance is essential. To protect prefinished wood flooring, ultra-violet curable acrylate coatings 100% solids are used. Even if coatings are increasingly performant, scratches formation is unavoidable, especially for soft substrates such as wood. To ensure

good appearance over time, self-healing coatings can be prepared. Several self-healing strategies are reported in the literature and they are classified as extrinsic (vascular and capsules-based) or intrinsic.

Vascular extrinsic technology is based on capillaries network filled with healing agent [1]. The capillaries are produced by direct-ink writing. Then, the healing agent is infiltrated inside the capillaries [1]. During mechanical solicitation, the capillary is broken, and the healing agent is released inside the scratch. This technology is more difficult to apply for very fast inline processes, as used in the wood coating industry. Concerning the capsules-based technology, capsules containing self-healing agent are dispersed into the coating formulation, before being applied onto the substrates. Therefore, this technology might be applicable for the wood industry. The solicitation causing the scratch breaks the capsules and the healing agent fills the scratch. The capsules-based technology allows a totally autonomous healing (no heat or other external stimuli needed) but does not permit repeatable healing in the same area. The intrinsic technology consists in the inclusion of reversible bonds in the coating, which does not affect the application procedure and is suitable to a large range of polymers. At the opposite of capsules, intrinsic technology allows repeatable healing under external stimuli. As the repaired sections are usually subject to new scratches [1], even more for wood flooring products which may endure daily mechanical solicitation. For this reason, the ability to achieve repeatable healing is essential for wood coatings. Therefore, the intrinsic healing technology is the most appropriate for this application.

The self-healing property in intrinsic technology is ensured by reversible bonds which create dynamic network opening and reforming infinitely, with or without external stimuli. Reversible bonds are covalent bonds in reversible reaction, weak bonds, or molecular tangles [1–3]. The latter are spontaneous interactions, instead of bonds. Only chain mobility is required to observe self-healing behavior and no stimulus is necessary. After damage, putting in contact the edges of the scratch can be enough to observe self-healing [1]. This technology is appropriate for materials with high chain mobility such as hydrogels and silicones [1]. Because UV-curable flooring coatings are highly crosslinked, molecular tangles cannot be observed (low chain mobility).

Technologies with reversible covalent bonds such as Diels–Alder and disulfide bonds are also reported in the literature [1,3]. Disulfide bonds are less studied because of the odor associated with the thiol group. Self-healing using Diels–Alder bonds is widely described in literature [4–6]. Wudl F. et al. have developed a polymer with reversible cross-linking, using Diels–Alder reaction between furan and maleimide [4]. One of the drawbacks with Diels–Alder-based self-healing technology is the very high temperature of retro-Diels–Alder. Another drawback is the yellowing of the furan after heating [4]. Because covalent bonds have high binding energy (200–400 kJ/mol), the temperature needed to open the temporary network is high (100–150 °C) [1,7,8]. Heating the surface above 100 °C can overdried wood. The temperature of the thermal stimuli depends on the strength bond, Figure 1.
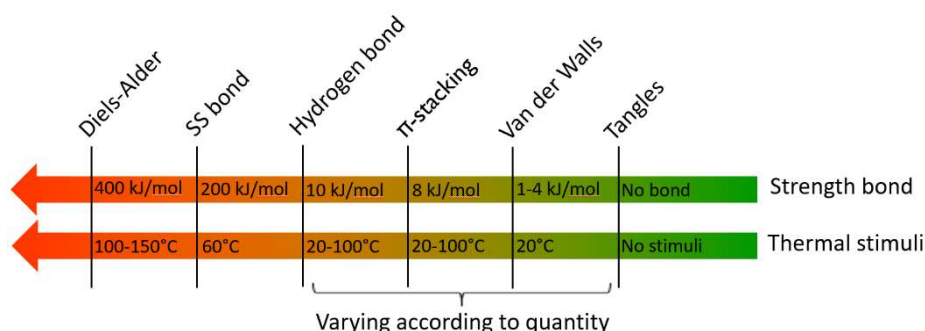

Figure 1. Diagram of reversible bonds according to stimuli needed to initiate self-healing.

The other reversible bonds that can be used are weak bonds, such as van der Waals interactions and hydrogen bonds. The strength bonding is low, so only a small amount of energy is needed to open the reversible weak bonds. For the wood coating application, mechanical properties are very important

to obtain scratch resistance. Stronger bonds increase the hardness of the material [9]. The strongest of the weak bonds is the hydrogen one, for that reason they are the most studied.

Several studies on self-healing polymers containing hydrogen bonds are present in the literature. For instance, Chen et al. developed a multiphase self-healing elastomer based on hydrogen bond composed of a polyamide grafted on polystyrene backbone [10]. In this case, polyamide, with hydrogen bonds, self-assembles in spheres inside the polystyrene matrix. Herbst et al. developed a self-healing polyisobutylene bearing hydrogen donor groups at the end of the main chain, stimulated by mechanical shearing instead of temperature [11]. Also, Liu et al. synthesized an oligomer that contains ureido groups, creating strong hydrogen bonds [12]. By varying the quantity of ureido groups, they determine that the concentration of hydrogen bonds impacts the temperature of the stimulus necessary to ensure self-healing. Similarly, Stadler et al. varied the number of hydrogen bonds by changing the binding group on a linear poly(butadiene) chain [13]. They concluded that the increase in the amount of hydrogen bonds in the material increases the temperature of the thermal stimulus initiating the self-healing behavior. Cortese et al. studied the quantity of hydrogen bonds in polymeric material [14]. Thymine (two intermolecular hydrogen bonds) or diaminotriazine (four intermolecular hydrogen bond) have been grafted on poly(propylene oxide) chains. They noticed that increasing the quantity of hydrogen bonds yield to an increase of the crystallinity of the polymer. Therefore, hydrogen bonds create a temporary network that increases the rigidity of the material. In return, this dense network inhibits chain mobility, so it is necessary to bring more energy (thermal in most cases) to undo this network and initiate self-healing. Moreover, self-healing UV curable polymers are also reported in the literature, mostly on polyurethane. Wang et al. developed UV curable polyurethane containing thiol-ene and Diels–Alder reversible bonds [15]. Liu et al. synthesized a UV curable and self-healable polyurethane oligomer from urethane prepolymer and hydroxyethylmethacrylate [16]. Finally, acrylate self-healing materials were developed but mostly on soft materials. Fan et al. studied the self-healing mechanism on acrylic elastomer [17]. They found that this self-healing is due to hydrogen bond between the carbonyl and the hydroxyl groups. The rare example of cross-linked self-healing polyacrylate used the 7-methacryloyoxycoumarin, which cross-links or open under light stimulus [18].

In summary, it is necessary to find the good quantity of hydrogen bonds to get a good self-healing property without inhibiting the chain mobility. For wood products, it is preferable to keep the thermal stimulus below 100 °C. UV-curable acrylate coatings used in wood flooring industry are highly cross-linked [19], thus with low chain mobility. The challenge is to obtain hard coating with enough chain mobility to reach self-healing at low temperature.

This paper presents the development of intrinsic self-healing acrylate UV curable coatings adapted to the wood industry. Hydrogen bond-based self-healing is selected to obtain self-healing at low temperature on rigid polymeric coatings. The formulation of self-healing coating combining stiffness and self-healing is presented in this paper. The impact of the quantity of hydrogen bonds on self-healing efficiency and physical properties is studied. Formulations with one or two hydroxyl components were developed. In wood application, mechanical properties are important to ensure resistant coating. Indeed, coatings must be hard to resist to mechanical solicitation, and flexible to resist wood swelling and shrinkage.

2. Materials and Methods

2.1. Materials

Table 1 presents a list of monomers and oligomers that were selected for this study. These components are among the less toxic acrylates containing alcohol or amide groups to create hydrogen bonding. The monomer must be liquid, transparent, and of a viscosity under 1000 cP. The oligomers must have more than two acrylate functions to guarantee the cross-linking, and a high quantity of alcohol or amide groups to ensure the self-healing property.

<div align="center">Table 1. Materials used in coatings formulation.</div>

Name	Description	Viscosity (cP)	Supplier	Function
HDDA	1,6-Hexanediol diacrylate	5	Canlak	Monomer
AHPMA	3-(Acryloyloxy)-2-hydroxypropyl methacrylate	44	Sigma-Aldrich	Monomer
PETA	Pentaerythritol triacrylate	1000	Sigma-Aldrich	Monomer
HEMA	2-Hydroxyethyl methacrylate	6	Sigma-Aldrich	Monomer
HPPA	2-Hydroxy-3-phenoxypropyl acrylate	200	Sigma-Aldrich	Monomer
	acrylic acid	Liquid	Sigma-Aldrich	Monomer
EDA	Epoxy diacrylate resin	30,000	Canlak	Oligomer
DGDA	Glycerol 1,3-diglycerolate diacrylate	10,000	Sigma-Aldrich	Oligomer
Ebecryl 4738	Aliphatic urethane acrylate, hard resin	35,000	Allnex	Acrylated allophanate oligomer
Ebecryl 4666	Unsaturated aliphatic urethane acrylate, hard resin	56,000	Allnex	Acrylated allophanate oligomer
Ebecryl 4740	Aliphatic urethane acrylate, flexible resin	8000	Allnex	Acrylated allophanate oligomer
HMPP	2-Hydroxy-2-methylpropiophenone	Liquid	Canlak	Photoinitiator absorbing at 240 nm

The reference coating, with no hydrogen bond, is a formulation composed of HDDA and EDA. The acrylate monomers with hydrogen bonding used are AHPMA, PETA, HEMA, HPPA and acrylic acid (Figure 2). The acrylate oligomers making hydrogen bonds are Ebecryl 4738, Ebecryl 4666, Ebecryl 4740 and DGDA. Because DGDA is a high viscosity monomer, it was used as a replacement to an oligomer.
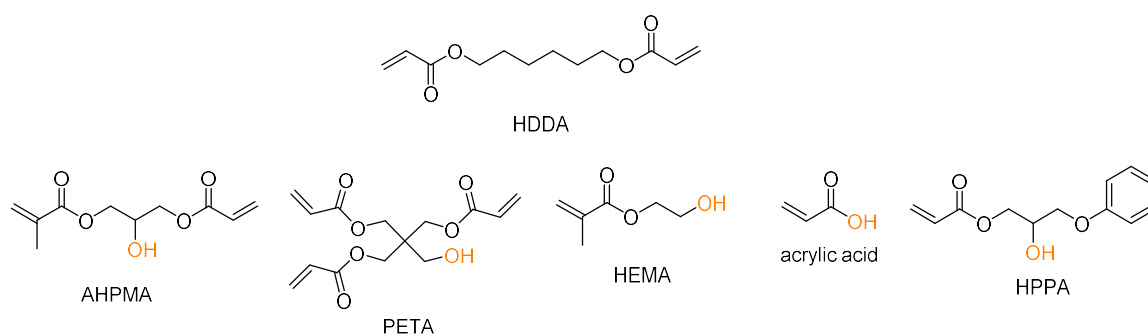
Figure 2. Structure of the acrylate monomers used in the formulations.

2.2. Coating Formulation and Application Procedure

Each formulation was prepared from one acrylate monomer, one acrylate oligomer and 3 w.% of HMPP photoinitiator described in Table 1. Oligomer, monomer and photoinitiator were added in order and mixed using Dissolver DISPERMAT LC30 (VMA, Reichshof, Germany). The speed was increased gradually up to 600 rpm to avoid bubbles formation. The ratio monomer/oligomer was set to obtain a viscosity between 2000–2500 cP at approximately 10 rpm, the target for roller coater application. The viscosity of the formulations, presented in Table 2, was measured using a CC25 rheometer (AMETEK Brookfield, Middleboro, MA, USA), the shear applied was 5 rpm for 2 min and 50 rpm for 2 min.

Table 2. Viscosity results (η) of one and two hydroxyl component formulations (components in bold carry alcohol groups).

n°	Monomer	Oligomer	% Oligomer	% Monomer	η at 5 rpm (cP)	η at 50 rpm (cP)
1	HDDA		82.5%	17.5%	2315	2486
2	**AHPMA**		70.0%	30.0%	2252	2514
3	**PETA**	EDA	64.9%	35.1%	20,157	2231
4	**HEMA**		82.5%	17.5%	2387	2522
5	**HPPA**		55.0%	45.0%	2267	2408
6	**Acrylic Acid**		82.9%	17.1%	2166	2301
7		**Ebecryl 4738**	85.0%	15.0%	2280	2549
8	HDDA	**Ebecryl 4666**	79.9%	20.1%	2031	2072
9		**Ebecryl 4740**	89.0%	11.0%	2237	2402
10		**DGDA**	85.0%	15.0%	2137	2178
11	**AHPMA**		65.0%	35.0%	2018	2106
12	**HEMA**	**Ebecryl 4738**	82.5%	17.5%	2336	2454
13	**HPPA**		54.9%	45.1%	2188	2254
14	**Acrylic Acid**		83.0%	17.0%	2257	2344
15	**AHPMA**		62.5%	37.5%	1976	2162
16	**HEMA**	**Ebecryl 4666**	78.9%	21.1%	2245	2351
17	**HPPA**		50.0%	50.0%	2135	2313
18	**Acrylic Acid**		82.0%	18.0%	2268	2358
19	**AHPMA**		77.5%	22.5%	2287	2447
20	**HEMA**	**Ebecryl 4740**	89.0%	11.0%	2255	2331
21	**HPPA**		67.5%	32.5%	2286	2457
22	**Acrylic Acid**		87.5%	12.5%	2315	2480
23	**AHPMA**		72.0%	28.0%	2192	2254
24	**HEMA**	**DGDA**	85.0%	15.0%	2109	2151
25	**HPPA**		60.0%	40.0%	2462	2438
26	**Acrylic Acid**		14.0%	86.0%	2165	2225

To study the impact of hydroxyl group concentration on self-healing behavior, formulations with one and two hydroxyl components were prepared. The reference coating (n° 1), with no hydroxyl group, is composed of HDDA and EDA. For the one component formulations, each hydroxyl acrylate monomer was mixed with EDA oligomer, and each hydroxyl acrylate oligomer was mixed with HDDA monomer. The components leading to promising results were then used for the two hydroxyl components formulations, each hydroxyl acrylate monomer was mixed with each hydroxyl acrylate oligomer.

Each coating formulation was applied using a square applicator film PA-5353 (BYK Additives & Instruments, Columbia, MD, USA) of 100 μm gap. Then, the films were cured under UV irradiation at 150 mW/cm^2 and 200 mJ/cm^2 and films of 60 μm thickness were obtained. A UV oven ATG 160 305 (Ayotte techno-gaz, Lourdes-de-Joliette, QC, Canada) was used, with a mercury light UV mac 10 (Nordson, Westlake, OH, USA) that emits at wavelengths in the range of 200–500 nm, and the conveyor speeds at 8 m/min. Three films of each formulation were prepared.

2.3. Physicochemical and Mechanical Characterization

2.3.1. Pendulum Damping Tests

To evaluate hardness and flexibility of the coatings, pendulum damping tests were performed. All coatings were characterized using a König pendulum hardness tester (BYK Additives & Instruments, Columbia, MD, USA) on glass panel as described in ASTM standard D4366 [20]. Wood substrate was not used because it is heterogenous and reduces the reproducibility. The coating film is applied on glass panel, the pendulum is placed on the coating and tilted up to 6°. The number of oscillations from 6° to 3° was measured. High number of oscillations relate to high hardness and low flexibility. If the coating is soft and/or flexible, the surface damps the pendulum and the number of oscillations

is low. To perform this test, three films of each formulation were applied on glass substrates. Three measurements were performed on each film.

2.3.2. Infrared Spectroscopy Measurements

Infrared spectroscopy was performed to evaluate both the hydrogen bonds quantity and the conversion. Each formulation (liquid) and films (polymerized) were characterized by Fourier transformation infrared spectroscopy (FT-IR) using a spectrometer (spectrum 400, Perkin Elmer, Woodbridge, ON, Canada), with an attenuated total reflectance (ATR) accessory. Thirty-two scans were recorded between 650 and 4000 cm^{-1}. Each spectrum was analyzed without any baseline correction. The characteristic stretching vibrations peaks are the carbonyl peak at 1710 cm^{-1}, the alkene at 1635 cm^{-1} and the bonded alcohol peak between 3340 and 3500 cm^{-1} (Figure 3). The quantity of hydrogen bonds can be followed using the alcohol peak.
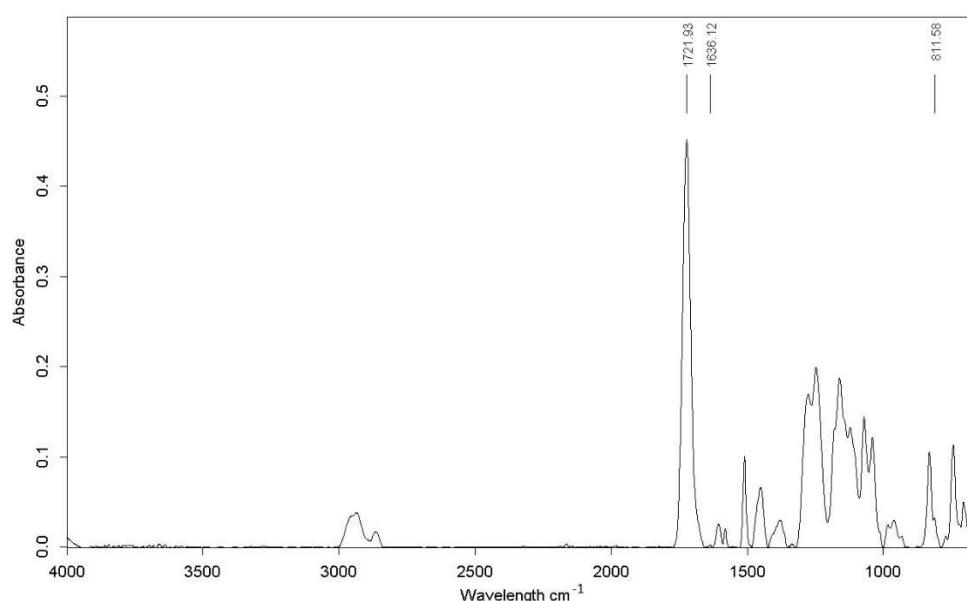
Figure 3. FT-IR spectrum of HDDA-EDA coating.

The conversion yield was calculated using carbonyl and alkene peaks intensity (Equation (1)). The calculation used is presented in Furtak–Wrona's paper [21].

$$\Pi = \left(1 - \frac{A_{\text{acryl}} \times A^0_{\text{ref}}}{A^0_{\text{acryl}} \times A_{\text{ref}}}\right) \times 100 \tag{1}$$

A_{acryl} is the absorption of the acrylate peak for cured films, A^0_{acryl} is the absorption of the acrylate peak for uncured formulations, A_{ref} is the absorption of the reference peak of cured films and A^0_{ref} is the absorption of the reference peak of uncured formulations. The reference peak is the carbonyl one (stretching at 1710 cm^{-1}) and the acrylate peaks are the alkene ones (stretching at 1635 cm^{-1} and twisting at 810 cm^{-1}). It can be noted that the presence of the peak at 1635 cm^{-1} can also be an indication of amine groups, as well as aromatic for the 810 cm^{-1} peak. Consequently, the 810 cm^{-1} peak was used for coating containing amine groups and 1635 cm^{-1} for the those containing aromatic groups to prevent amine or aromatic influence.

2.3.3. Dynamic Mechanical Analysis Measurements (DMA)

DMA was used to measure the glass transition temperature and cross-linking density of the films. DMA experiments were performed from 30 °C (or 0 °C for coatings with low glass transition

temperature) to (T_g + 70 °C) at 3 °C/min, the force track selected was 125%, the preload 0.1 N, the strain 0.2% and the frequency was set to 1 Hz. To ensure the quality of the preparation, coatings were cut using a CO_2 Laser Machine Center at 500 W (LMC-2000 from Beam Dynamic, Edgar, WI, USA). The sample size selected was 2.5 cm × 0.5 cm. The glass transition occurs during a range of temperature. The maximum of loss modulus indicates the middle temperature of glass transition (Figure 4). The cross-liking density was calculated using the minimum of storage modulus, with the following equation:

$$D_c = \frac{E'}{3 \times R \times T}$$ (2)

where E' is the storage modulus in the rubbery plateau at T_g + 50 °C, R is the gas constant, and T is the temperature at T_g + 50 °C.
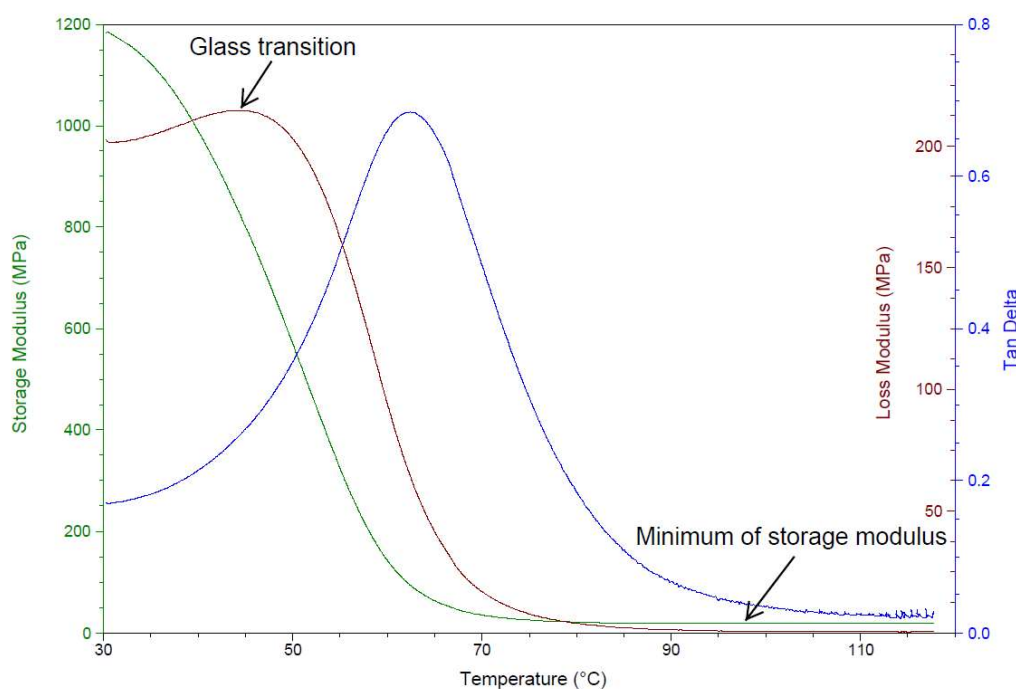
Figure 4. DMA curve indicating the glass transition temperature and the minimum of storage modulus.

2.4. Self-Healing Characterization

As wood is heterogenous, self-healing tests were performed on metallic substrates to ensure better reproducibility. Self-healing was studied by two methods: the gloss recovery to characterize the visual aspect, and the scratch recovery for the mechanical aspect. For both tests, the deformation applied is in the elastic-plastic domain. The self-healing efficiency was calculated from the gloss recovered after heating in the first case and from the scratch depth in the second case. To discuss the results, statistical analysis was performed with the Tukey method. Scanning electron microscopy images were taken with the JSM-6360LV (JEOL, Tokyo, Japan), at 15 kV irradiation. Samples were coated with gold, under argon atmosphere.

2.4.1. Self-Healing Characterization by Gloss Measurements

Damaged surfaces were prepared using the Abrasion and Washability Tester (Elcometer 1720, Warren, MI, USA). As in the standard ISO 11998 [22] the speed was set at 37 cycles/min. The abrasive tool completed 5 cycles. The abrasion pad used was the Scotch Brite 7447B (from 3M, Saint Paul, MN, USA). Gloss measurements were taken before and after damage and then after 2 h in the oven at 80 °C. They were performed with the micro-TRI-gloss from BYK, which measures gloss at 20°, 60°

and 80°. For semi-gloss coatings, the gloss used is at 60°. From the gloss measurements, the self-healing efficiency was calculated with the following equation:

$$Self\text{-}healing \ (\%) = \frac{gloss_{\text{healed coating}} - gloss_{\text{damaged coating}}}{gloss_{\text{virgin coating}} - gloss_{\text{damaged coating}}} \times 100 \tag{3}$$

To estimate the depth of the deformation, profilometry measurements were performed on the coatings after abrasion. The white laser on the station Micromesure CHR 150 was used (STIL, Aix-en-Provence, France). The measurement information was taken by the SurfaceMap software. Then MontainMap software was operated to analyze the images obtained. To improve scratch depth calculation quality, a leveling is applied on the images. Then, robust Gaussian filter was operated to ignore surface roughness. Finally, the surface parameters were calculated by the software, as presented in Figure 5, the "S_v" parameter represents the deepest point on the image and is considered as the scratch depth.
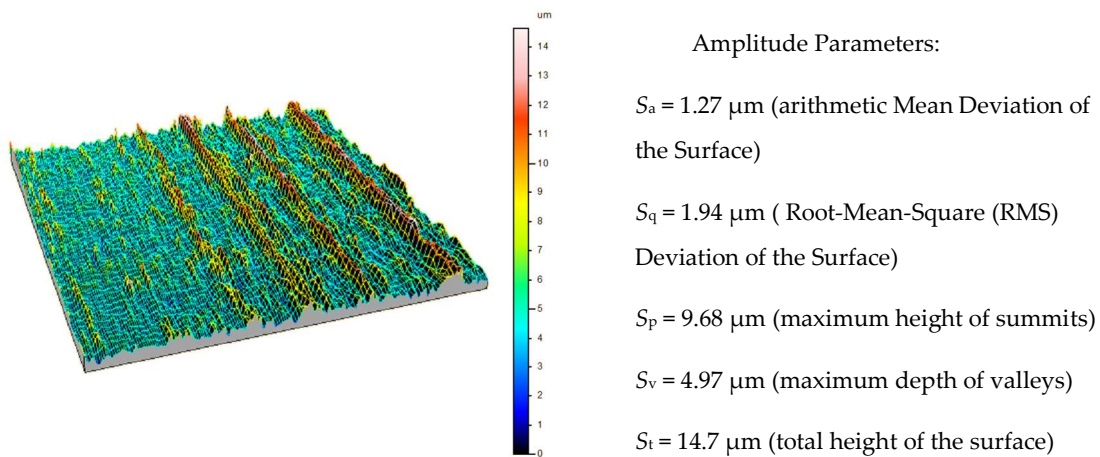

Amplitude Parameters:

S_a = 1.27 µm (arithmetic Mean Deviation of the Surface)

S_q = 1.94 µm (Root-Mean-Square (RMS) Deviation of the Surface)

S_P = 9.68 µm (maximum height of summits)

S_v = 4.97 µm (maximum depth of valleys)

S_t = 14.7 µm (total height of the surface)

Figure 5. Profilometry image of the coating n° 1 after 5 cycles of abrasion.

2.4.2. Self-Healing Characterization by Scratch Depth Measurements

Micro Combi Tester (MCT, Anton Paar, Graz, Austria) produces scratches with controlled depth. A Rockwell C diamond tip with a radius of curvature of 200 µm was used. Three scratches were performed at a constant load, for 3 mm length, at a speed of 6 mm/min. The load was selected to obtain scratch depth of approximately 5 µm, for that, all coatings were damaged using a 5 N load, only the n° 13 needed 7, 5 N load to produce 5 µm depth scratch.

Scratch depth was measured by optical profilometry. The equipment used was the ContourGTI profilometer (Bruker, Billerica, MA, USA), using the VSI mode, 5× lens, and 2× multiplier. Measures were taken with the white LED, the threshold at 1%, speed measurement at 1×, 10 µm of back scan, and 25 µm of scan length. To characterize the entire scratch, stitching was set with 20% overlap to improve measurement quality. Profilometry measurements give the average scratch depth, before and after healing at 80 °C for 2 h. The difference in scratch depth before and after healing indicates the self-healing efficiency of the coating (4).

$$Self\text{-}healing \ efficiency \ (\%) = \frac{Depth_{\text{healed coating}} - Depth_{\text{damaged coating}}}{Depth_{\text{damaged coating}}} \times 100 \tag{4}$$

3. Results and Discussion

3.1. Formulations Selection

3.1.1. Formulation with One Hydroxyl Component

Formulations, and films, were prepared with one component containing hydroxyl groups. König hardness pendulum measurements were performed to select the best coatings in term of hardness and flexibility. The results are presented in Table 3.

Table 3. Hardness results of one hydroxyl component formulations (components in bold carry alcohol groups).

n°	Monomer	Oligomer	Hardness Pendulum (osc)
1	HDDA	EDA	81 ± 1
2	**AHPMA**	EDA	90 ± 6
3	**PETA**	EDA	123 ± 3
4	**HEMA**	EDA	25 ± 5
5	**HPPA**	EDA	17 ± 1
6	**Acrylic acid**	EDA	102 ± 2
7	HDDA	**Ebecryl 4738**	96 ± 5
8	HDDA	**Ebecryl 4666**	100 ± 5
9	HDDA	**Ebecryl 4740**	35 ± 5
10	HDDA	**DGDA**	101 ± 2

To be applicable to wood industry, coating must resist to mechanical solicitation and to wood dimensional changes. Therefore, coatings must be hard and flexible, as the reference coating n° 1. To reach this mechanical behavior, the coatings selected are the ones with pendulum hardness around 80 oscillations. It can be noticed that the coating n° 3 shows a high hardness. As the monomer is trifunctional, the coating is highly crosslinked. Nevertheless, this result is too high and indicates low flexibility for a sealer, which is not suitable. As a result, this monomer was not used for the following tests. The results for the coating n° 9 indicate low hardness. Therefore, the Ebecryl 4740 oligomer was not used for the rest of the study. The coatings n° 4 and n° 5 lead to low hardness. For these coatings it is the monomer part which was studied. As the oligomer part is dominant, the pendulum damping results can be improved using different oligomers in the formulation.

In summary, the components kept for the second part of the study are the monomers AHPMA, HEMA, HPPA and acrylic acid, and the oligomers Ebecryl 4738, Ebecryl 4666 and DGDA. To develop formulations with two hydroxyl components each monomer was mixed with each oligomer.

3.1.2. Formulation with Two Hydrogen Bond Components

Formulations with two components containing hydroxyl groups were prepared. The results are presented in Table 4.

To perform the measurements the pendulum is placed on the coating surface, thus the topography impacts the results. If the sample is not completely flat, the reproducibility of the result decreases. This is notable for the coating n° 17, the roughness (because of orange peel effect) causes high standard deviation. Photography of coating n° 17 with orange peel effect, and coating n° 16 which is smooth, are presented in Figure 6.

Table 4. Hardness results of two hydrogen bond components formulations, (components in bold carry alcohol groups).

n°	Monomer	Oligomer	Hardness Pendulum (osc)
11	**AHPMA**		70 ± 5
12	**HEMA**	**Ebecryl 4738**	81 ± 5
13	**HPPA**		97 ± 3
14	**Acrylic acid**		130 ± 1
15	**AHPMA**		126 ± 2
16	**HEMA**	**Ebecryl 4666**	104 ± 3
17	**HPPA**		72 ± 7
18	**Acrylic acid**		122 ± 5
19	**AHPMA**		112 ± 5
20	**HEMA**	**DGDA**	96 ± 1
21	**Acrylic acid**		111 ± 7

(**a**)   (**b**)
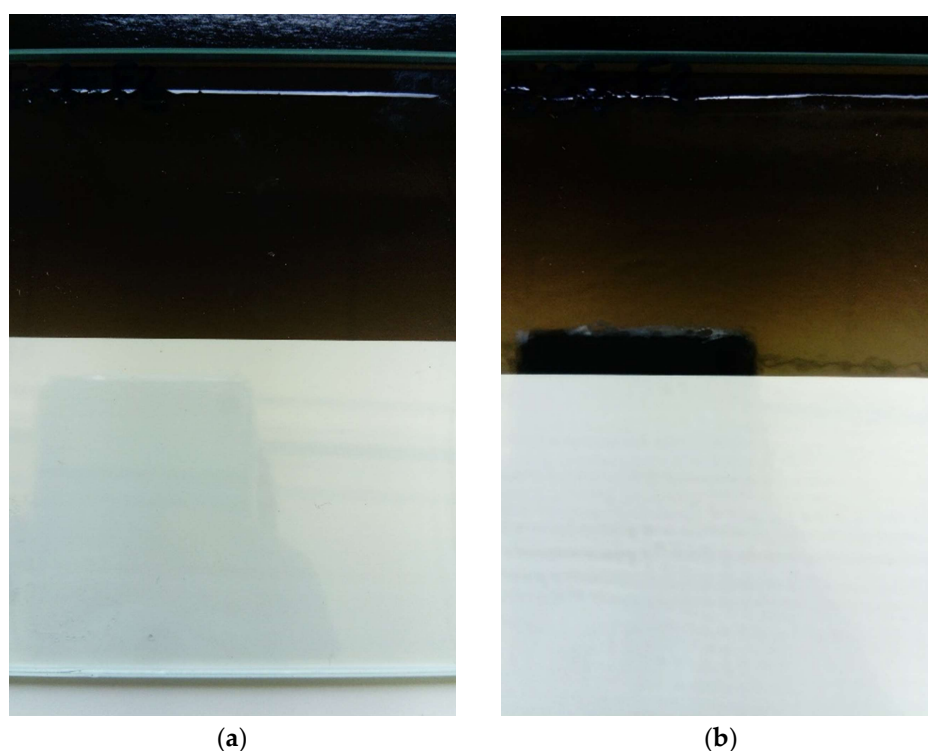
Figure 6. Photography of smooth coating (**a**) and coating with orange peel effect (**b**). Coatings are applied on glass panel.

As stated previously, the hardness target is around 80 oscillations. The coatings with AHPMA, acrylic acid monomers and DGDA as oligomer (n° 11, 14, 15, 18–21) have hardness pendulum results too high, which indicates low flexibility. Indeed, the reference coating is easy to manipulate. At the opposite, these coatings broke apart when they are removed from the substrate. This lack of flexibility makes them unusable for wood application. DGDA is a bifunctional monomer but is very viscous (8000–1200 cP) so it was used as a replacement for the oligomer portion of the formulation. This monomer contains three hydroxyl groups. Thus, a high quantity of intra- and inter-molecular hydrogen bonds are created, and the dynamic network induces rigidity.

On the other hand, the coatings with HEMA and HPPA monomers indicate hardness results applicable for the wood products industry.

The following studies sections present the physicochemical characterization and the self-healing measurements of seven formulations (n° 1, 4, 5, 12, 13, 16, 17); the reference coating and the ones with HEMA and HPPA monomers, varying the oligomer part to evaluate the impact of hydrogen bond quantity.

3.2. Physicochemical and Mechanical Characterization

3.2.1. Fourier Transformation Infrared Spectroscopy

Infrared spectroscopy experiments were performed with two purposes: evaluate the relative quantity of hydrogen bonds and the conversion. As the quantity of hydrogen bonds increase, the alcohol peak shifts from 3500 to 3340 cm^{-1}. Indeed, the bond strength impact the vibrations and induces this shift [23]

It is notable on Figure 7 that the reference film (n° 1) displays no sign of hydrogen bonding. In fact, if the alcohol groups are free, the alcohol peak is expected to be between 3590 and 3650 cm^{-1}. For the films prepared with one hydroxyl component (n° 4 and n° 5), the infrared spectrum shows a large peak at 3500 cm^{-1}, which confirms the presence of hydrogen bonding. For the films with two hydroxyl components (n° 12, 13, 16, 17), the large alcohol peak is shifted to 3340 cm^{-1}. This shift indicates the augmentation of hydrogen bonds quantity [24]. These results confirm that the quantity of hydrogen bonds in the cured films increases with the quantity of acrylate component containing alcohol groups. Then, coatings with higher hydrogen bond quantity should have higher self-healing efficiency.
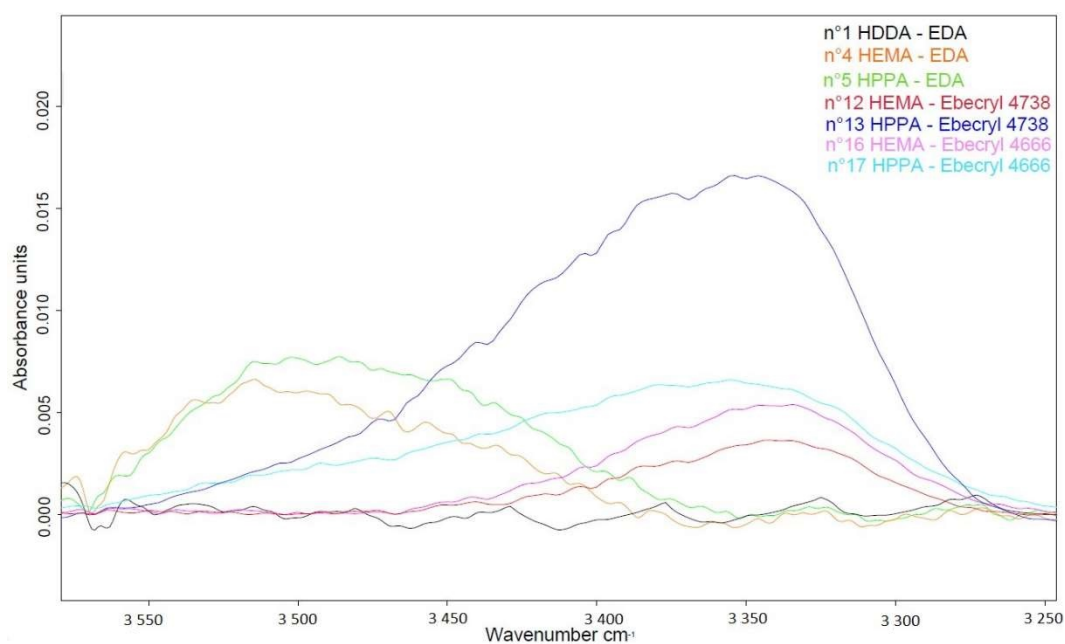

Figure 7. FT-IR spectrum of coatings n° 1, 4, 5, 12, 13, 16, 17, in the alcohol stretching region.

Conversion yields were calculated using the formula presented in Equation (1). Conversion yield results are presented in Table 5.

It is notable that the lower conversion yield is obtained for the coating n° 1, which has no hydrogen bonds ability. This is coherent with the hypothesis that hydrogen bonds create preorganization of monomers that increase the polymerization [25]. For formulations with high functionality due to Ebecryl oligomer (coatings n° 12 to n° 17), the polymeric network stiffens faster, so the conversion yield is low. The highest conversion yield is obtained for coating n° 5. The conversion yield is induced by the structure, the number of acrylate functions and the polymerization rate of the components in the formulation.

Table 5. Conversion yield results measured by FT-IR spectroscopy (components in bold carry alcohol groups).

n°	Formulation	C=C Acrylate Peak Used (cm^{-1})	Conversion Yield (%)
1	HDDA–EDA	1635	49
4	**HEMA**–EDA	1635	85
5	**HPPA**–EDA	1635	88
12	**HEMA–Ebecryl 4738**	810	70
13	**HPPA–Ebecryl 4738**	810	67
16	**HEMA–Ebecryl 4666**	810	85
17	**HPPA–Ebecryl 4666**	810	66

3.2.2. Dynamic Mechanical Analysis

Glass transition temperature and cross-linking density were measured with DMA. Results are presented in Table 6.

Table 6. Glass transition temperature and crosslinking density measured by DMA (components in bold carry alcohol groups).

n°	Formulation	T_g (°C) = max(E'')	Cross-Linking Density (mol/m^3)
1	HDDA–EDA	43 ± 3	620 ± 108
4	**HEMA**–EDA	42 ± 0.5	630 ± 94
5	**HPPA**–EDA	37 ± 1	622 ± 42
12	**HEMA–Ebecryl 4738**	78 ± 2	3268 ± 89
13	**HPPA–Ebecryl 4738**	55 ± 1	1963 ± 163
16	**HEMA–Ebecryl 4666**	72 ± 2	3154 ± 124
17	**HPPA–Ebecryl 4666**	53 ± 3	1801 ± 112

The coatings with EDA (n° 1, 4, 5) have low T_g values and cross-linking densities. This is due to the oligomer functionality. EDA has two acrylate functions, instead of three and four functions for the oligomers Ebecryl 4738 and Ebecryl 4666 respectively. The low cross-linking density of the coatings n° 4, 5 is coherent with their high conversion yield, as explain previously. It is notable that the coatings with HEMA and acrylated allophanate oligomers (n° 12, 16) have the highest T_g value and cross-linking density observed. Moreover, the HPPA monomer (coatings n° 5, 13, 17) provides lower cross-linking density than HEMA. This could be explained by steric hindrance provided by the phenoxy group of HPPA, which hinders the chain mobility. This difference between HEMA and HPPA monomer coatings is not observable in the conversion yield results. This means that steric hindrance (causing decrease of cross-linking) have less effect on conversion yield than molar functionality.

At low temperature, the polymer is in the glass state as the polymeric chains do not have enough thermal energy. Above the glass transition temperature, the polymer is in the rubber state, there is chain mobility. The highest T_g is 78 °C for the coating n° 12. Chain mobility is necessary to ensure self-healing, so the coatings were all heated at 80 °C for the self-healing characterizations. This temperature is usable in the daily life (for example with a hair dryer) and is low enough to not damage wood. Also, high T_g is useful to get hard coating. In the following section, the self-healing property is studied to observe if a high cross-linking density prevents the self-healing.

3.3. Self-Healing Characterization

According to previous analysis, the coatings studied for self-healing behavior were the reference one (n° 1), the ones with HEMA (n° 4, 12, 16) and HPPA monomers (n° 5, 13, 17). These coatings were selected according to damping pendulum results which indicate hardness and flexibility (Section 3.1. Formulations Selection).

3.3.1. Self-Healing Characterization by Gloss Measurements

To evaluate the self-healing property, five abrasion cycles were performed as indicated in the Material section. The self-healing efficiency, measures by the gloss recovered after heating, was calculated with the Equation (3). The results are presented in Table 7. According to S_v parameter on profilometry measurements of abraded coatings, five cycles of abrasion produce damages of about 5 μm depth.

Table 7. Gloss measurements (at 60°) before abrasion, after abrasion and after heating (components in bold carry alcohol groups).

n°	Formulation	Gloss before Abrasion	Gloss after Abrasion	Gloss after Heating	Self-Healing Efficiency (%)	Groups of Results
1	HDDA–EDA	124	98	99	4	C
4	**HEMA**–EDA	123	103	120	85	A
5	**HPPA**–EDA	119	103	108	31	B
12	**HEMA–Ebecryl 4738**	116	87	111	83	A
13	**HPPA–Ebecryl 4738**	123	101	107	27	B
16	**HEMA–Ebecryl 4666**	119	75	90	34	B
17	**HPPA–Ebecryl 4666**	119	101	109	44	B

The reference coating (n° 1) has no reversible bond, but present 4% of self-healing, it belongs to C group of the statistical analysis. This recovery represents the stress relaxation occurring at β and glass transitions [26]. Therefore, for all coatings, a part of the gloss recovery is not due directly to self-healing behavior. Concerning the visual aspect of abrasion, coatings were considered in this study as self-healing if the abrasions are invisible to naked eye after heating. It was observed that abrasions are not visible anymore above 80% of gloss recovery.

It is notable that coatings with HPPA monomer (n° 5, 13, 17) do not have self-healing property, either for one hydroxyl component formulation than for two hydroxyl components formulations. It could be due to steric hindrance of the phenyl group. The Ebecryl 4666 oligomer (n° 16, 17) does not show self-healing behavior. Information about its exact structure is not available, however it may be due to lower quantity of hydrogen bonds than Ebecryl 4738. Each coating with the HPPA monomer and with Ebecryl 4666 oligomer all belongs to group B according to statistical analysis. The HEMA-EDA and HEMA-Ebecryl 4738 coatings (n° 4, 12) show self-healing with respectively 85% and 83% of healing efficiency. These coatings have T_g values of 30 and 70 °C, respectively. It was expected that coatings with higher hydrogen bonding would have higher self-healing efficiency. In this case, both coatings are heated at the same temperature (80 °C), so the coating n° 4 is heated 50 °C above its T_g value, instead of 10 °C for the coating n° 12. The polymeric network of the coatings n° 4 gains more chain mobility than the coatings n° 12. This explains the high self-healing efficiency of coating n° 4 despite it contain only one hydroxyl component.

The two self-healing coatings are in group A in statistics. The Tukey method indicates that results between self-healing coating (n° 4 and 12) are significantly different from coatings in groups B and C. Also, the reference coating (n° 1) is the only one in group C, which confirms that hydrogen bonds in formulation impact the results of self-healing efficiency.

To illustrate the self-healing effect, SEM images are presented in Figure 8 of reference coating (n° 1) and self-healing coating (n° 12).
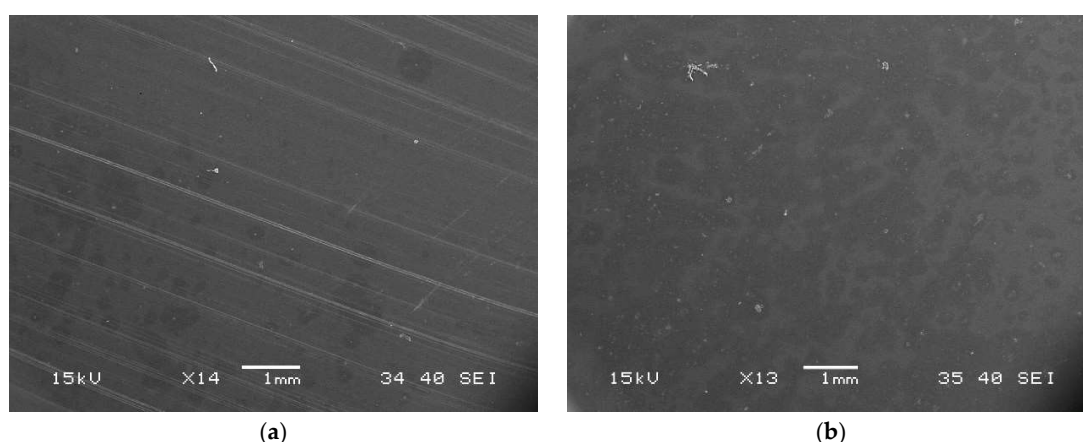
Figure 8. SEM images of reference coating (**a**) and self-healing coating n° 12 (**b**) after heating 2 h at 80 °C.

3.3.2. Self-Healing Characterization by Scratch Depth Measurements

Self-healing was characterized by measuring scratch depth recovery. The coatings studied were the same than the ones for the self-healing characterization by gloss measurements. Scratches of 5 μm depth were prepared and scratch depth was measured before and after healing. The results are presented in Table 8.

Table 8. Scratch recovery after 5 μm scratch and heating 2 h at 80 °C (components in bold carry alcohol groups).

n°	Formulation	Scratch Depth before Healing (μm)	Scratch Depth after Healing (μm)	Self-Healing Efficiency (%)	Presence of Scratches after Heating	Groups of Results
1	HDDA–EDA	4.2 ± 0.6	1 ± 0.1	75	Scratches visible	C
4	**HEMA**–EDA	5.9 ± 0.2	0.4 ± 0.1	91	Scratches not visible	B
5	**HPPA**–EDA	Fracture from 1 μm deep	No healing	0	Scratches visible	–
12	**HEMA–Ebecryl 4738**	5.5 ± 0.4	0 ± 0.1	100	Scratches not visible	A
13	**HPPA–Ebecryl 4738**	5.0 ± 0.2	Peel from the substrate	–	Scratches visible	–
16	**HEMA–Ebecryl 4666**	4.3 ± 0.3	0.4 ± 0.1	89	Scratches visible	B
17	**HPPA–Ebecryl 4666**	6.1 ± 0.7	Peel from the substrate	–	Scratches visible	–

The results are in agreement with the study of self-healing characterization by gloss, as only two coatings with HEMA (n° 4, 12) provide visible healing. The Tukey statistical analysis leads to the same groups of results as previously. The steric hindrance in the formulation with HPPA (n° 5, 13, 17) prevents healing and the Ebecryl 4666 oligomer (n° 16, 17) do not provide self-healing behavior. As in the previous study, a stress relaxation during heating is observed. This causes 75% of healing on the reference coating (n° 1), which has no reversible bonds. This recovery is high because the scratches performed have ductile behavior. In this case, the elastic and plastic stresses can be partially released with heating [27]. In this test the coating HEMA-Ebecryl 4738 (n° 12) is totally self-healing, the scratches disappeared, as it can be seen on Figure 9. At the opposite, for the reference coating (n° 1), scratches are still observable after heating. These results are also noticeable on surface profiles made from profilometry data, Figure 10. On the reference coating the scratch after heating is still visible even if the depth decreases by 75%. On the self-healing coating (n° 12) the surface after heating is totally flat. Self-healing efficiency measurements were difficult to perform for coatings n° 5, 13, 17 as the contacting tip induces plastic flow (pile up), making profilometry measurements difficult. More specially, for coatings n° 13, 17, these pile up "hides" the scratch from the profilometric LED.

Moreover, after heating, these two samples lose the adherence ad were partially removed from the substrate, making reliable depth measurements impossible. Also, the coating HPPA-epoxy acrylate oligomer (n° 5) fractures from 1 µm scratch deep. During fracture, small parts of the coating are removed, and scratch depth cannot be measured (Appendix A).
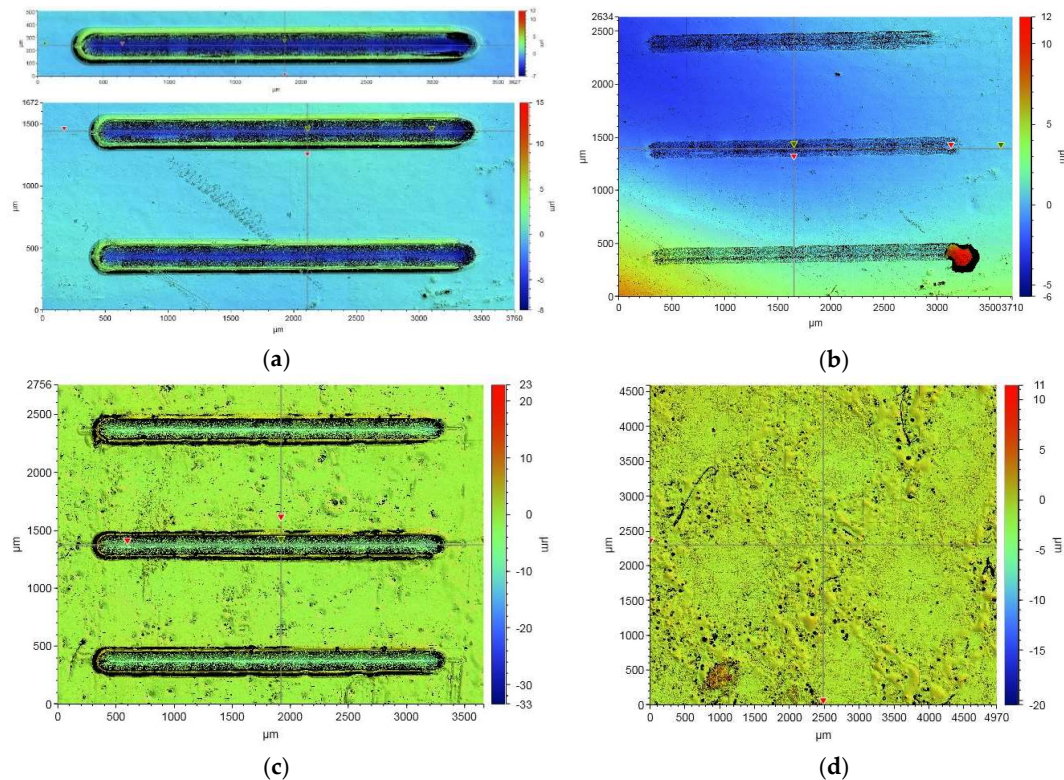

Figure 9. Images from profilometry measurement of coatings n° 1 before (**a**) and after (**b**) heating and n° 12 before (**c**) and after (**d**) heating 2 h at 80 °C.
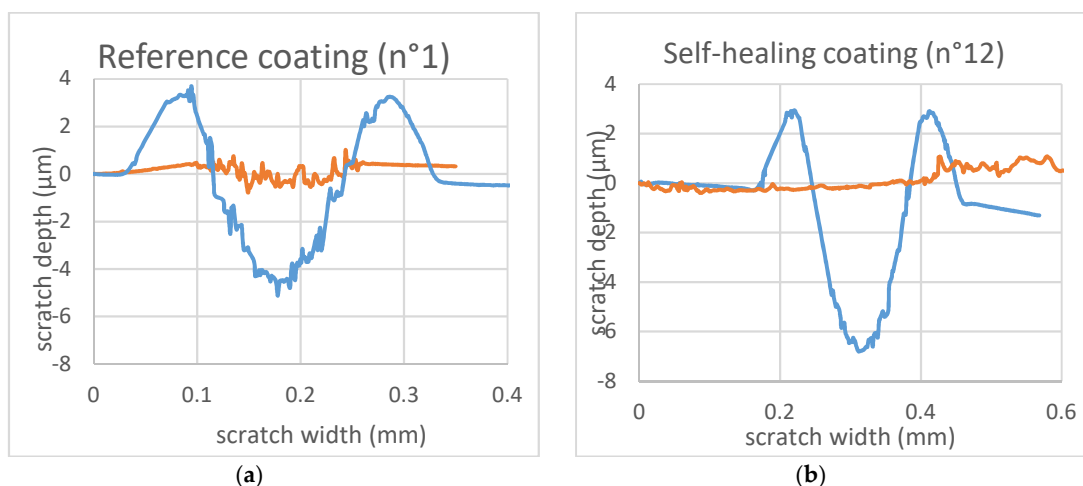
Figure 10. Scratch track profiles from profilometry data, before (blue) and after (orange) heating, of the reference coating (**a**) and self-healing coating (**b**).

The Tukey analysis confirms that reference coating (n° 1) is the only that do not present self-healing, and coating n° 12 is the most self-healing. Tukey test do not included coatings containing HPPA as there is no exact value of self-healing efficiency. It is notable that coating n° 4 was in the A group for the characterization by gloss measurement and is in B group for the characterization by scratch depth

measurement. This could be due to the number of coatings which is different between the two tests (n° 5, 13, 17 were not taking in account for the second Tukey test). This could also indicate that coating n° 4 is less self-healing than coating n° 12.

To illustrate the self-healing, Figure 11 presents SEM photography of coating n° 1, 12 after the heating.
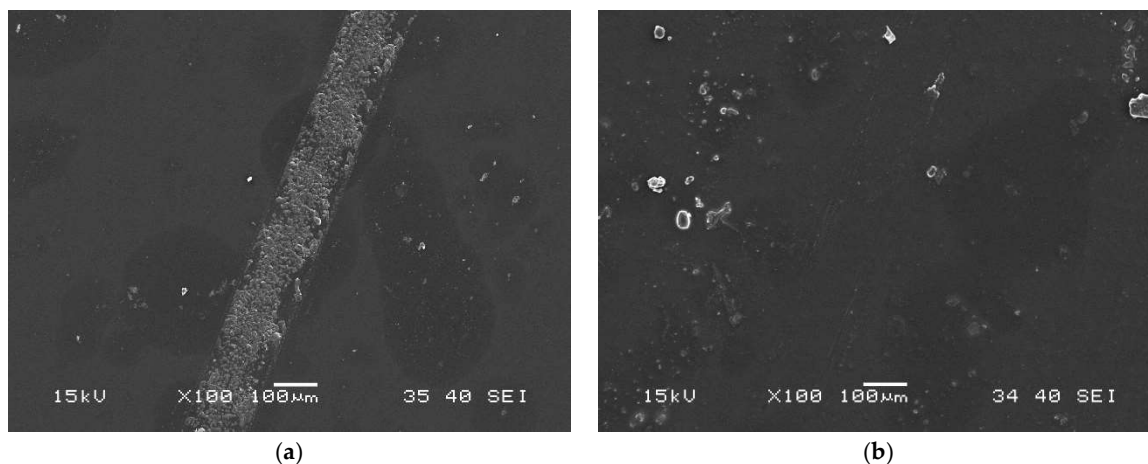
Figure 11. SEM images of reference coating (**a**) and HEMA-Ebecryl4738 (**b**) after 2 h heating at 80 °C.

It is notable that the coating n° 12 providing maximum of self-healing is also the one with the highest cross-linking density. This is possible because the formulation has very low steric hindrance and a high quantity of hydrogen bonds. At T_g, the self-healing occurs. Moreover, this coating has good hardness and flexibility to be applied on wood. This coating is innovative because it combines high cross-linking density and healing temperature under 100 °C. Indeed, as presented in the literature part, coatings with high mechanical properties usually need a thermal stimulus around 150 °C to ensure self-healing. In this case, the low steric hindrance makes the chain mobility, necessary to the self-healing, possible at only 80 °C. The second part of the study focus on the impact of the addition of a second monomer on the hardness and self-healing parameters of the resulting coatings.

4. Conclusions

In this article, UV curable acrylate coatings with self-healing behavior based on hydrogen bonding were developed. To be applicable in the wood flooring industry, coatings must be hard and flexible. The challenge is that self-healing efficiency depends on chain mobility, but UV curable coatings are highly cross-linked.

The quantity of hydrogen bonds was analyzed by FT-IR and revealed that the oligomer part of the formulation brings the highest quantity of hydrogen bonds. Hydrogen bonds yielded to a preorganization of the molecular network, which assisted the polymerization and thus increased the conversion yield. Also, high functionality decreased the polymerization. DMA measurements demonstrated that the formulation functionality and steric hindrance affected the T_g value and cross-linking density. Self-healing characterization experiments revealed that stress relaxation occurs during heating, even for coatings with no reversible bond. Self-healing occurred only for coatings with low steric hindrance and high quantity of hydrogen bond. Results indicated that the coating HEMA-Ebecryl 4738 (n° 12) possessed good self-healing efficiency, with heating at T_g value, while presenting high cross-linking. With 81 oscillations of pendulum damping, this coating has the hardness and flexibility suitable for wood industry. It is not necessary to heat up to 100 °C to observe self-healing. In conclusion, to combine self-healing property and high cross-linking, it is important to prevent steric hindrance.

Appendix A

(**a**) (**b**)

Figure A1. HEMA—EDA profilometry images before (**a**) and after (**b**) heating.

(**a**) (**b**)
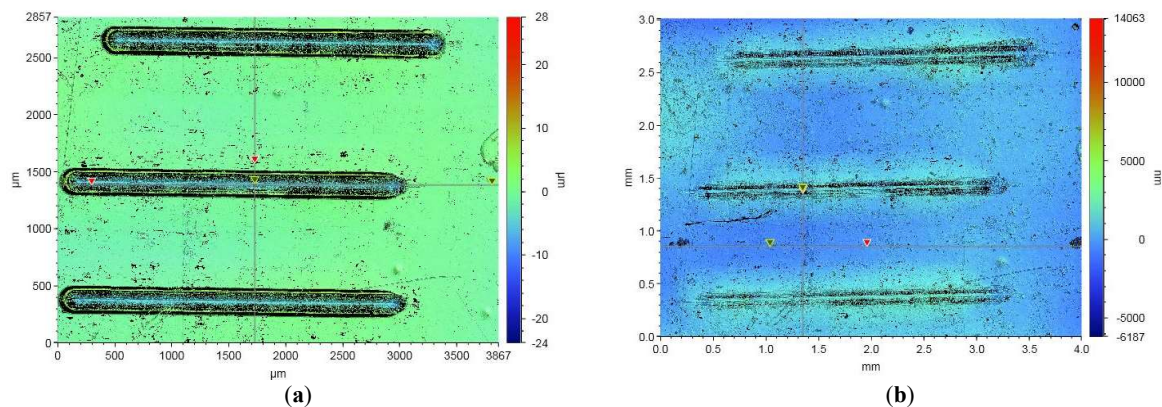
Figure A2. HEMA—Ebecryl 4666 profilometry images before (**a**) and after (**b**) heating.
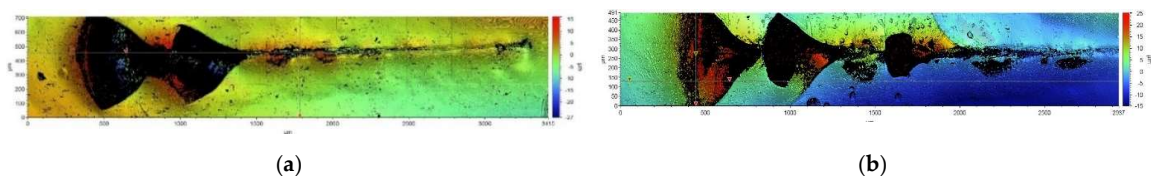

(**a**) (**b**)

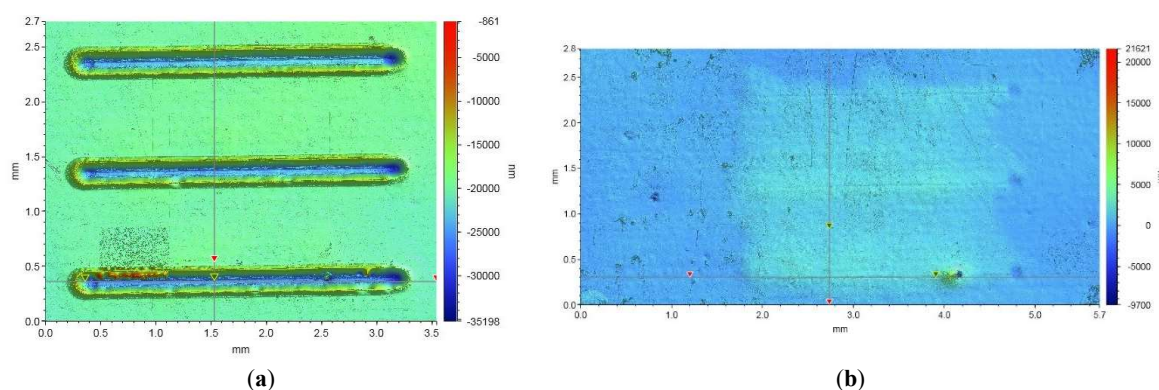**Figure A3.** HPPA—EDA profilometry images before (**a**) and after (**b**) heating.

Figure A4. HPPA—Ebecryl 4738 profilometry images before (**a**) and after (**b**) heating.
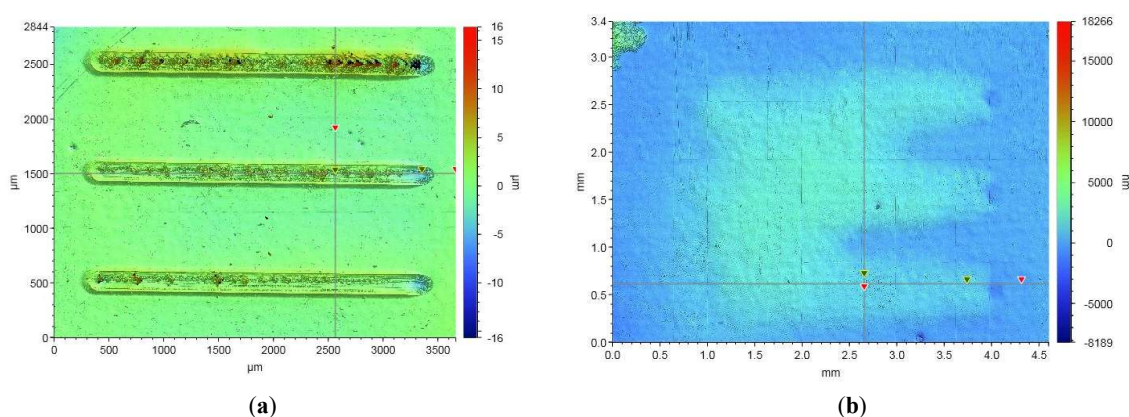

Figure A5. HPPA—Ebecryl 4666 profilometry images before (**a**) and after (**b**) heating.

References

1. Blaiszik, B.J.; Kramer, S.L.B.; Olugebefola, S.C.; Moore, J.S.; Sottos, N.R.; White, S.R. Self-healing polymers and composites. *Annu. Rev. Mater. Res.* **2010**, *40*, 179–211. [CrossRef]
2. Zhong, N.; Post, W. Self-repair of structural and functional composites with intrinsically self-healing polymer matrices: A review. *Compos. Part A Appl. Sci. Manuf.* **2015**, *69*, 226–239. [CrossRef]
3. Herbst, F.; Döhler, D.; Michael, P.; Binder, W.H. Self-healing polymers via supramolecular forces. *Macromol. Rapid Commun.* **2013**, *34*, 203–220. [CrossRef]
4. Chen, X.; Dam, M.A.; Ono, K.; Mal, A.; Shen, H.; Nutt, S.R.; Sheran, K.; Wudl, F. A thermally re-mendable cross-linked polymeric material. *Science* **2002**, *295*, 1698–1702. [CrossRef]
5. Murphy, E.B.; Bolanos, E.; Schaffner-Hamann, C.; Wudl, F.; Nutt, S.R.; Auad, M.L. Synthesis and characterization of a single-component thermally remendable polymer network: Staudinger and stille revisited. *Macromolecules* **2008**, *41*, 5203–5209. [CrossRef]
6. Jo, Y.Y.; Lee, A.S.; Baek, K.-Y.; Lee, H.; Hwang, S.S. Thermally reversible self-healing polysilsesquioxane structure-property relationships based on Diels-Alder chemistry. *Polymer* **2017**, *108*, 58–65. [CrossRef]
7. White, S.R.; Sottos, N.R.; Geubelle, P.H.; Moore, J.S.; Kessler, M.R.; Sriram, S.R.; Brown, E.N.; Viswanathan, S. Autonomic healing of polymer composites. *Nature* **2001**, *409*, 794–797. [CrossRef]
8. Wilson, G.O.; Porter, K.A.; Weissman, H.; White, S.R.; Sottos, N.R.; Moore, J.S. Stability of second generation grubbs' alkylidenes to primary amines: Formation of novel ruthenium-amine complexes. *J. Für Prakt. Chem. Chem. Ztg.* **2009**, *351*, 1817–1825. [CrossRef]
9. Boyer, D.B.; Chalkley, Y.; Chan, K.C. Correlation between strength of bonding to enamel and mechanical properties of dental composites. *J. Biomed. Mater. Res.* **1982**, *16*, 775–783. [CrossRef]
10. Chen, Y.; Kushner, A.M.; Williams, G.A.; Guan, Z. Multiphase design of autonomic self-healing thermoplastic elastomers. *Nat. Chem.* **2012**, *4*, 467–472. [CrossRef]

11. Herbst, F.; Schröter, K.; Gunkel, I.; Gröger, S.; Thurn-Albrecht, T.; Balbach, J.; Binder, W.H. Aggregation and chain dynamics in supramolecular polymers by dynamic rheology: Cluster formation and self-aggregation. *Macromolecules* **2010**, *43*, 10006–10016. [CrossRef]

12. Liu, R.; Yang, X.; Yuan, Y.; Liu, J.; Liu, X. Synthesis and properties of UV-curable self-healing oligomer. *Prog. Org. Coat.* **2016**, *101*, 122–129. [CrossRef]

13. Hilger, C.; Stadler, R. Cooperative structure formation by combination of covalent and association chain polymers: 4. Designing functional groups for supramolecular structure formation. *Polymer* **1991**, *32*, 3244–3249. [CrossRef]

14. Cortese, J.; Soulié-Ziakovic, C.; Tencé-Girault, S.; Leibler, L. Suppression of mesoscopic order by complementary interactions in supramolecular polymers. *J. Am. Chem. Soc.* **2012**, *134*, 3671–3674. [CrossRef]

15. Wang, Z.; Liang, H.; Yang, H.; Xiong, L.; Zhou, J.; Huang, S.; Zhao, C.; Zhong, J.; Fan, X. UV-curable self-healing polyurethane coating based on thiol-ene and Diels-Alder double click reactions. *Prog. Org. Coat.* **2019**, *137*, 105282. [CrossRef]

16. Liu, J.; Cao, J.; Zhou, Z.; Liu, R.; Yuan, Y.; Liu, X. Stiff self-healing coating based on UV-curable polyurethane with a "hard core, flexible arm" structure. *ACS Omega* **2018**, *3*, 11128–11135. [CrossRef]

17. Fan, F.; Szpunar, J. The self-healing mechanism of an industrial acrylic elastomer. *J. Appl. Polym. Sci.* **2015**, *132*. [CrossRef]

18. Abdallh, M.; Hearn, M.T.W.; Simon, G.P.; Saito, K. Light triggered self-healing of polyacrylate polymers crosslinked with 7-methacryloyoxycoumarin crosslinker. *Polym. Chem.* **2017**, *8*, 5875–5883. [CrossRef]

19. Müller, B. *Coatings Formulation*; Vincentz Network: Hannover, Germany, 2011; ISBN 978-3-86630-891-6.

20. *ASTM D4366-16 Standard Test Methods for Hardness of Organic Coatings by Pendulum Damping Tests*; ASTM: West Conshohocken, PA, USA, 2016.

21. Furtak-Wrona, K.; Kozik-Ostrówka, P.; Jadwiszczak, K.; Maigret, J.E.; Aguié-Béghin, V.; Coqueret, X. Polyurethane acrylate networks including cellulose nanocrystals: A comparison between UV and EB- curing. *Radiat. Phys. Chem.* **2018**, *142*, 94–99. [CrossRef]

22. *ISO 11998:2006 Paints and Varnishes—Determination of Wet-Scrub Resistance and Cleanability of Coatings*; International Organization for Standardization: Geneva, Switzerland, 2006.

23. Silverstein, R.M.; Webster, F.X.; Kiemle, D.J. Spectrometric identification of organic compounds seventh edition. *J. Chem. Educ.* **2005**, *39*, 546. [CrossRef]

24. Tsubomura, H. Nature of the Hydrogen Bond. III. The Measurement of the infrared absorption intensities of free and hydrogen-bonded oh bands. Theory of the increase of the intensity due to the hydrogen bond. *J. Chem. Phys.* **1956**, *24*, 927–931. [CrossRef]

25. Jansen, J.F.G.A.; Dias, A.A.; Dorschu, M.; Coussens, B. Fast monomers: Factors affecting the inherent reactivity of acrylate monomers in photoinitiated acrylate polymerization. *Macromolecules* **2003**, *36*, 3861–3873. [CrossRef]

26. Higgenbotham-bertolucci, P.R.; Gao, H.; Harmon, J.P. Creep and stress relaxation in methacrylate polymers: Two mechanisms of relaxation behavior across the glass transition region. *Polym. Eng. Sci.* **2001**, *41*, 873–880. [CrossRef]

27. Lörinczová, I.; Decker, C. Scratch resistance of UV-cured acrylic clearcoats. *Surf. Coat. Int. Part B Coat. Trans.* **2006**, *89*, 133–143. [CrossRef]